Jurnal Teknologi

Full Paper

STAND AGE MODEL FOR MAPPING SPATIAL DISTRIBUTION OF RUBBER TREE USING REMOTELY SENSED DATA IN KEDAH, MALAYSIA

Iqbal Putut Ash Shidiq, Mohd Hasmadi Ismail*

Department of Forest Production, Faculty of Forestry, Universiti Putra Malaysia, 43400 UPM, Serdang, Selangor, Malaysia

*Corresponding author
mhasmadi@upm.edu.my

Article history
Received
4 July 2015
Received in revised form
8 November 2015
Accepted
7 March 2016

Graphical abstract

Abstract

This study attempt to develop stand age model of rubber tree by using remote sensing data. Rubber tree is one of the important biomass that has been considered as the essential part in global warming reduction plan due to its beneficial carbon sequestration capability. The spatial distribution of rubber tree based on different age was most highlighted as the focus of this study. Felda Lubuk Merbau in state of Kedah has been selected as a study area and Landsat 8 OLI-TIRS data was utilized to map rubber tree and differentiate them based on age group. The relationship between vegetation indices namely NDVI, SAVI and EVI to different age stages of rubber tree were discussed.

Keywords: Rubber tree identification, rubber tree age classification, remote sensing, vegetation indices

1.0 INTRODUCTION

The issue of climate change becomes more popular nowadays. The impacts of this phenomenon have been globally perceived and actions to overcome this matter have been initiated [1]. Greenhouse gas, especially CO_2 emitted from industrial, transportation and land conversion has become the main agent causing the global warming [2, 3, 4].

Forest ecosystem plays an important role as the global carbon pool, because the dynamic cycle of terrestrial carbon dominantly occurs here [5, 6]. As one of the terrestrial forest ecosystem, rubber tree plays an important role in climate change mitigation. The tree itself can be functioned both as the carbon absorber and provider (in the form of biomass) [7].

On the other hand, the conversion from natural forest to rubber plantation in significant amount has become as serious issue in Southeast Asia. This condition greatly affects water balance, carbon cycle and biodiversity [8]. Therefore, mapping and monitoring become important to estimate the level of impact from rubber expansion to ecological condition.

The remote sensing system is very suitable to be utilized in this application. The excellence of remote sensing in capturing earth surface features will tackle the commonly time and labor consuming problems in this kind of study. Various types of vegetation indices generated from remote sensing image such as NDVI, SAVI and EVI, have been used by many researches to develop model and to analyses vegetation features like phenology, biomass and carbon cycle [9].

This paper will focus on analyzing the distribution of rubber tree, especially in Felda Lubuk Merbau, Kedah Malaysia. The rubber tree distribution map will be generated by model based on relationship between spectral reflectance of Landsat 8 image and rubber tree stand parameter. The other objective of this study is to examine the fittest model which can describe the relationship between spectral characteristics and vegetation indices derived from remote sensing image with different age group of rubber tree

2.0 LITERATURE REVIEW

The Pará rubber tree (*Hevea brasiliensis*) naturally comes from Amazon Basin of South America. Rubber has become a major forest commodity. The expansion of rubber plantation is very rapid, especially in China

and Southeast Asia region [10, 11]. The high demand of rubber product is one of the reasons [12, 13]. The other reasons might relate with the recent important issues, namely climate change and renewable energy. The rubber plantation has been considered as the essential part towards global warming reduction plan due to its carbon sequestration capability. With its economic life and carbon storage capability, rubber trees considered as secure sources of green energy [7].

3.0 METHODOLOGY

Several main steps before the data is ready to be analyzed include image pre-processing, image processing and model generation.

3.1 Study Area

This study has been carried out in the Felda Lubuk Merbau, which located in the north-western part of Peninsular Malaysia, within the administrative region of Sik in the State of Kedah. The entire location of this site is between 5°57'54" to 6°2'6" North and between 100°40'48" to 100°44'24" East. The area of this site is about 2,906.41 Ha and almost 50% of the land has been planted with rubber in 2014. Figure 1 shows the location of study area

Figure 1 Location of study area

3.2 Remote Sensing Images

Landsat 8 OLI-TIRS satellite image has been used in this study. The level 1 product of this satellite image was downloaded from http://glovis.usgs.gov/. This is the latest series of Landsat satellite program launched in 2013 and carried two sensors: the Operational Land Imager (OLI) and the Thermal Infrared Sensor (TIRS). The OLI sensor has nine bands with 30 m spatial resolution for all bands (coastal/aerosol, blue, green, red, NIR, SWIR-1, SWIR-2 and Cirrus), except the 15 m panchromatic band, while the TIRS has two thermal bands (TIR 1 and TIR 2) with 100 m spatial resolution. The temporal resolution of this remote sensing system is 16 days. The image acquisition date was on March 2nd, 2015. The selection was based on minimum cloud cover percentage and compesate with field campaign period (Figure 2).

Figure 2 Selected Landsat 8 image

3.3 Ground Measurement

Field work was conducted in February 2015. A total 196 samples has been taken from eight plots. 30 x 30 m rectangular plots were designed to accommodate the spatial resolution of Landsat image. Those plots were randomly distributed based on different age group of the tree (Figure 3). The plots were placed in two different land characteristics such as lowland flat area and hilly with slope area. The field work includes measurement of tree stand parameters like diameter at breast height (DBH) and tree height (Figure 4).

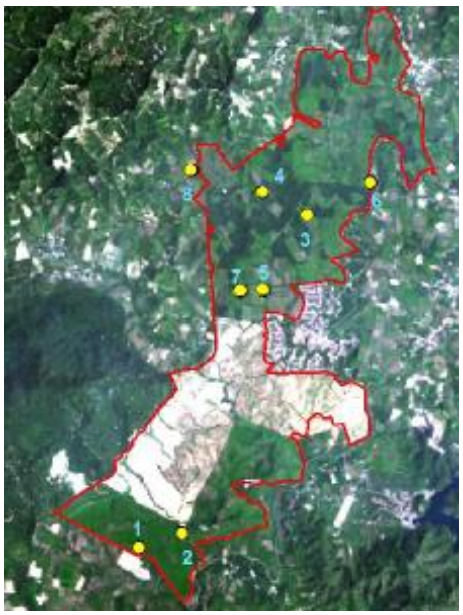

Figure 3 Sample distribution

3.4 Image Pre-Processing

The pre-processing includes radiometric correction process. The final result of this process is image with Top of Atmosphere (TOA) reflectance value which more suitable in generating vegetation indices. The conversion of Landsat DN value to TOA reflectance with sun angle correction is using the following formula:

$$\rho\lambda = (M_\rho Q_{cal} + A_\rho)/\sin(\theta_{SE}) \quad (1)$$

where:

$\rho\lambda$ = TOA planetary reflectance with sun angle correction
M_ρ = Band-specific multiplicative rescalling factor from metadata
Q_{cal} = Digital Number (DN)
A_ρ = Band-specific additive rescalling factor from metadata
θ_{SE} = Local sun elevation angle

Figure 4 DBH measurement

3.5 Image Processing

There vegetation indices namely Normalized Difference Vegetation Index (NDVI), Soil-Adjusted Vegetation Index (SAVI) and Enhanced Vegetation Index (EVI) were derived from Landsat 8 image with the following formula [14, 15, 16, 17]:

$$NDVI = (NIR - Red)/(NIR + Red) \quad (2)$$

$$SAVI = (NIR - Red)/(NIR + Red + L) * (1 + L) \quad (3)$$

$$EVI = G * [(NIR - Red)/(NIR + C1 * Red - C2 * Blue + L)] \quad (4)$$

where:

NIR = Landsat 8 near infrared band (Band 5)
Red = Landsat 8 red band (Band 4)
L = Soil adjustment factor based on vegetation density
C1 and C2 = Coefficient for aerosol scattering correction
Blue = Landsat 8 blue band (Band 2)

3.6 Model Generation

The statistical-based correlation analysis has been widely used to develop model and examine the relationship between satellite image spectral reflectance and radar backscattering to stand parameter or biomass [18, 19]. The predictor variables are the individual Landsat 8 OLI bands and three vegetation indices (NDVI, SAVI and EVI) (Table 1). The Pearson's correlation coefficient is used to determine the level of relationship between predictor and response variables.

Table 1 List of predictor variables

Variables	Utilized bands	Label
Individual Landsat 8 band	Band 1-9	B1-B9
NDVI	(Band 5 - Band 4)/(Band 5 + Band 4)	VI1
SAVI	(Band 5 - Band 4)/(Band 5 + Band 4 + 0.5)*(1+0.5)	VI2
EVI	2.5*[(Band 5 - Band 4)/(Band 5 + (6*Band 4) - (7.5*Band 2) + 1)]	VI3

4.0 RESULTS AND DISCUSSION

4.1 Characteristics of Samples

A total 196 samples has been taken from eight plots. We can differentiate the trees based on four age groups; 5, 10, 15 and 20 years old tree. The average DBH ranged from 47.57 to 84.31 cm, while the average height ranged from 6.58 to 7.27 m (Table 2 and Figure 5).

Table 2 Summary of samples

Plot no.	Number of sample	Age group	Average DBH (cm)	Average height (m)
1	26	10	84.31	7.08
2	11	10	72.06	6.98
3	10	15	71.79	7.15
4	29	15	75.88	7.12
5	30	20	77.36	7.34
6	31	5	52.05	6.93
7	30	20	70.15	7.27
8	29	5	47.57	6.58
Total	196			

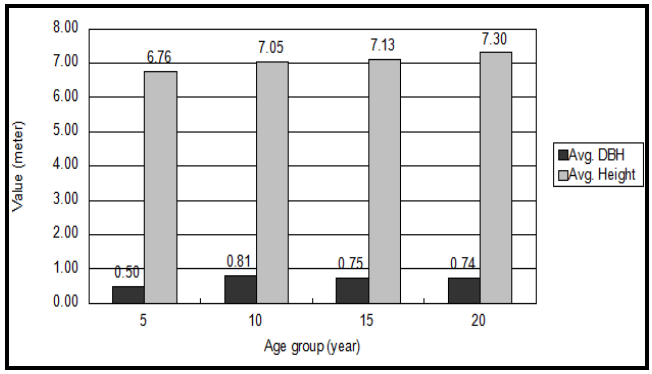

Figure 5 Variations in DBH and height within different tree age group

Based on the logaritmic regression, there is no strong correlation between each stand parameter (Table 3). The strongest relation is between age group and DBH. But with 0.2498 on its R-squared, it is not convincing enough to state the relationship between age group and DBH.

Table 3 Relationship between stand parameters

	Age	DBH	Height
Age			
DBH	y=17.645Ln(x)+25.485 R^2 = 0.2498		
Height	y=33.535Ln(x)-52.899 R^2 = 0.1724	y=98.941Ln(x)-125.49 R^2 = 0.1385	

4.2 NDVI, SAVI and EVI Characteristics

The SAVI and EVI showed similar on minimum value, while NDVI and EVI are very close in maximum value (Table 4). Figure 5 depicts the map of each VI. The SAVI and EVI show similar arrangements. On the other hand, the NDVI map shows greener color objects (Figure 6).

Table 4 NDVI, SAVI and EVI value of Landsat 8

Vegetation Index	Min	Max	Mean	SD
NDVI	0.008155	0.829335	0.648678	0.117276
SAVI	0.004724	0.603855	0.399462	0.077788
EVI	0.005459	0.890689	0.561399	0.121601

4.3 Relationship Between Stand Parameters and Spectral Reflectance

In general, the relationships between stand parameters and spectral reflectance are weak. All of the correlation coefficients are showing insignificant value (Table 5). However, all Landsat 8 visible and short-wave infrared bands are having a slightly stronger correlation with the age group. The highest correlation coefficient (R^2=0.4912) was found between age group and Band 6 (SWIR-1; 1.566-1.651 µm).

The similar condition also found in previous research. Weak correlations between stand age, DBH, height and Landsat 5 TM bands were experienced by Suratman in 2005. The only difference is that negative relationships were produced in his study. I his study, the highest correlation coefficient value (R^2 = -0.6) were found between DBH and Band 4 (NIR; 0.75-0.90 µm). The difference characteristic of bands between Landsat 5 and 8 was probably caused this. A further study is required for a better understanding on how different tree stages respond to Landsat spectral bands.

4.4 Stand Age Group Modeling

The model developed in this study is an individual model which solely based on stand age and spectral reflectance relationship. There are three models being proposed based on the strongest relationship (Table 6).

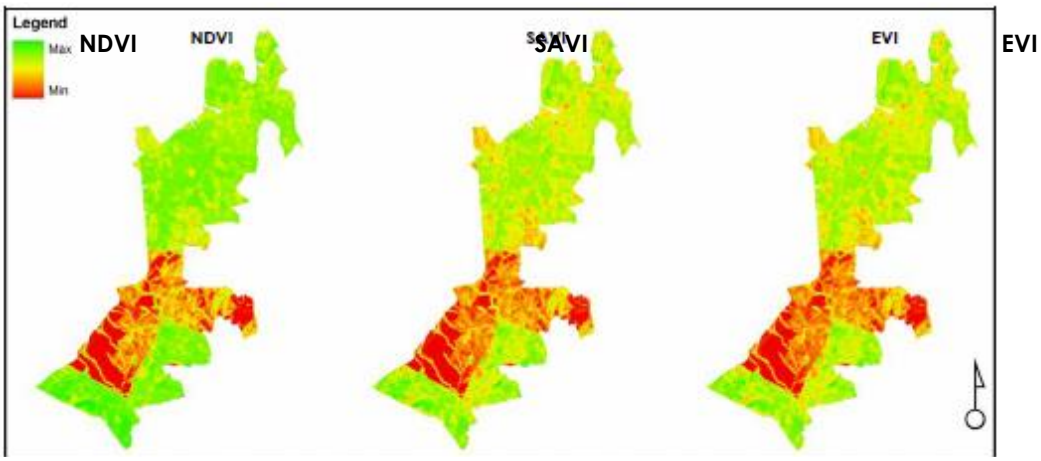

Figure 6 NDVI, SAVI and EVI map generated from Landsat 8 image

Table 5 Correlations between stand parameters and spectral reflectance

	Band 1	Band 2	Band 3	Band 4	Band 5	Band 6	Band 7	NDVI	SAVI	EVI
Age group	0.4295	0.4586	0.4135	0.4099	0.0886	0.4912	0.4335	0.2874	0.1308	0.1464
DBH	0.1131	0.104	0.0111	0.0603	0.053	0.0569	0.0524	0.0577	0.0271	0.0387
Height	0.06	0.0566	0.0261	0.0228	0.0838	0.0167	0.0146	0.0232	0.0011	0.0231

Table 6 Comparison of stand age model

Model No.	Formula	R^2
1	$y=0.0001x^{[(2-0.0034)x+0.0983]}$	0.4586
2	$y=0.0007x^{[(2-0.0168)x+0.2317]}$	0.4912
3	$y=0.0004x^{[(2-0.0099)x+0.1142]}$	0.4335

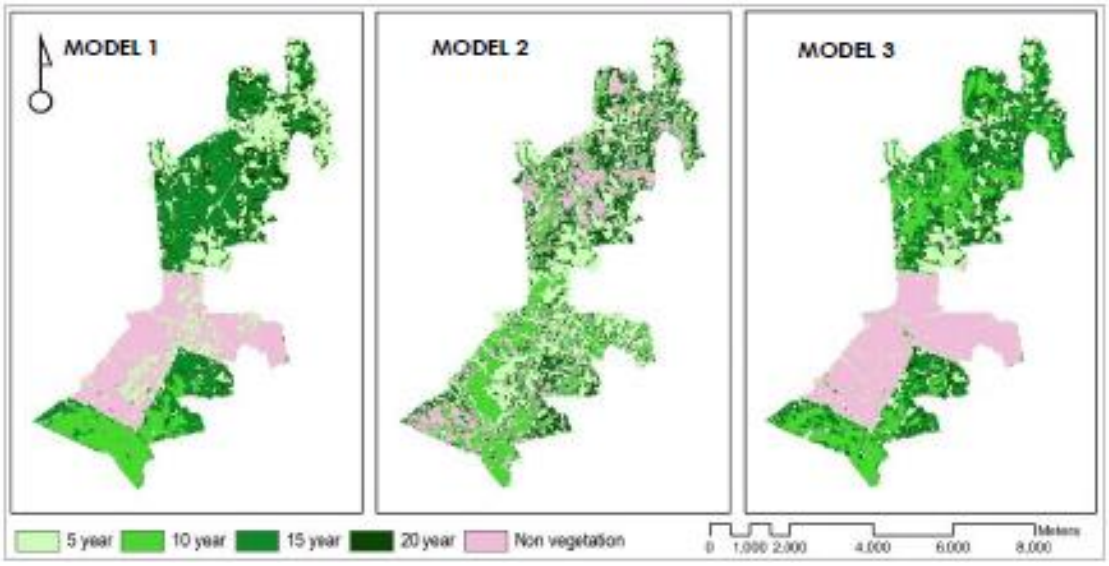

Figure 7 Rubber trees distribution map generated from models

Three rubber distribution maps were generated based on the model (Figure 7). Each map shows different characteristics. The map form Model 2 seems to have the least accuracy. Several non-vegetation areas in the center to the south were misclassified as rubber. Meanwhile, the other two models classify those areas as non-vegetation. Model 1 showed a dominant distribution of 15 years rubber in north, while Model 3 has 10 years rubber prevalently spread in the same area.

5.0 CONCLUSION

This study demonstrated the capability of Landsat 8 OLI-TIRS spectral bands to determine different stages of rubber trees. The conclusions for this research are as follows:

1. There no significant correlations between stand parameters, Landsat 8 OLI-TIRS bands and vegetation indices. However, slightly better relationships were founded between rubber tree age group, visible and shortwave bands.
2. Rubber distribution maps based on different age group were successfully generated from the model. However, there are still some misclassifications which might cause under- or over-estimation.

These three models are not yet to be validated. A further study on combining more than one spectral band and vegetation index is required to improve the correlation and increase the accuracy of results.

References

[1] Dessler, Andrew. 2012. *Introduction to Modern Climate Change*. Cambrige University Press, New York, NY, USA.

[2] Neelin, David J. 2011. *Climate Change and Climate Modelling*. Cambrige University Press, New York, NY, USA.

[3] Prentice, I. C., Farquhar, G. D., Fasham, M. J. R., Goulden, M. L., Heimann, M., Jaramillo, V. J., Kheshgi, H. S., Le Quéré, C., Scholes, R. J., Walace, D. W. R. 2001. The Carbon Cycle and Atmospheric Carbon Dioxide in Houghton, J. T., Ding, Y., Griggs, D. J., Noguer, M., van der Linden, P. J., Dai, X., Maskell, K., Johnson, C. A. (Eds.). *Climate Change 2001: The Scientific Basis*, Cambridge University Press, Cambridge. 183-237.

[4] Ravindranath, N.H. and Ostwald, M. 2008. *Carbon Inventory Methods: Handbook for Greenhouse Gas Inventory, Carbon Mitigation and Roundwood Production Projects*. Springer Science, Business Media B.V.

[5] Dong, J., Kaufmann, R. K., Myneni, R. B., Tucker, C. J., Kauppi, P. E., Liski, J., Buermann, W., Alexeyev, V., Hughes, M. K. 2003. Remote Sensing Estimates Of Boreal And Temperate Forest Woody Biomass: Carbon Pools, Sources, and Sinks. *Journal of Remote Sensing of Environment*. 84(2003): 393-410. Elsevier Science Inc.

[6] Turner, D. P., Guzy, M., Lefsky, M. A., Ritts, D. W., van Tuyl, S., Law, E. B. 2004. Monitoring Forest Carbon Sequestration with Remote Sensing and Carbon Cycle Modelling. *Journal of Environmental Management*. 33(4): 457-466. Springer-Verlag, New York.

[7] Krukanont, P. and Prasertsan, S. 2004. Geographical Distribution Of Biomass And Potential Sites Of Rubber Wood Fired Power Plants In Southern Thailand. *Journal of Biomass and Biology*. 26(2004): 47-59. Elsevier Ltd.

[8] Senf, C., Pflugmacher, D., van der Linden, S., Hostert, P. 2013. Mapping Rubber Plantations and Natural Forest in Xishuangbanna (Southwest China) Using Multi-Spectral Phenological Metrics from MODIS Time Series. *Remote Sensing*. 5: 2795-2812.

[9] Shidiq, I. P. A., Mohd Hasmadi,I., & Kamarudin, N. 2014. Initial Results Of The Spatial Distribution Of Rubber Tress In Peninsular Malaysia Using Remotely Sensed Data For Biomass Estimate. *IOP Conference Series: Earth and Environmental Science*. 18. doi:10.1088/1755-1315/18/1/012135.

[10] Li, Z., Fox, J. M. 2011. Rubber Tree Distribution Mapping in Northeast Thailand. *International Journal of Geosciences*.. 573-584.

[11] Li, Z., & Fox, J. M. 2012. Mapping Rubber Tree Growth In Mainland Southeast Asia Using Time-Series MODIS 250 m NDVI and Statistical Data. *Applied Geography*. 32(2): 420-432. doi:10.1016/j.apgeog.2011.06.018.

[12] Dong, J., Xiao, X., Sheldon, S., Biradar, C., & Xie, G. 2012. Mapping Tropical Forests And Rubber Plantations In Complex Landscapes By Integrating PALSAR And MODIS Imagery. *ISPRS Journal of Photogrammetry and Remote Sensing*. 74: 20-33. doi:10.1016/j.isprsjprs.2012.07.004.

[13] Dong, J., Xiao, X., Chen, B., Torbick, N., Jin, C., Zhang, G., & Biradar, C. 2013. Mapping Deciduous Rubber Plantations Through Integration Of PALSAR And Multi-Temporal Landsat Imagery. *Remote Sensing of Environment*. 134: 392-402. doi:10.1016/j.rse.2013.03.014.

[14] Rouse, J. W., R. H. Haas, J. A. Schell, and D. W. Deering. 1973. Monitoring Vegetation Systems in the Great Plains with ERTS. Third ERTS Symposium, NASA. SP-351 I:309-317

[15] Huete, A. R. 1988. A Soil-Adjusted Vegetation Index (SAVI). *Remote Sensing of Environment*. 25: 295-309.

[16] Liu, H. Q., Huete, A. R. A. 1995. Feedback Based Modification Of The NDV I To Minimize Canopy Background And Atmospheric Noise. *IEEE Transactions on Geoscience and Remote Sensing*. 33: 457-465.

[17] Matsushita, B., Yang, W., Chen, J., Onda, Y., Qiu, G. 2007. Sensitivity of the Enhanced Vegetation Index (EVI) and Normalized Difference Vegetation Index (NDVI) to Topographic Effects: A Case Study in High-Density Cypress Forest. *Sensors*. 7: 2636-2651.

[18] Suratman, M. Z. 2003. *Applicability of Landsat TM Data for Inventorying and Monitoring of Rubber (Hevea Brasiliensis) Plantations in Selangor, Malaysia: Lingkages to Policies*. Faculty of Forestry. The University of British Columbia.

[19] Hamdan, O., Aziz, H. K., Mohd Hasmadi, I. 2014. L-band ALOS PALSAR for Biomass Estimation of Matang Mangroves, Malaysia. *Remote Sensing of Environment*. 155: 69-78.